Monatsh Chem (2010) 141:1213–1221
DOI 10.1007/s00706-010-0393-2

ORIGINAL PAPER

DFT study of 1,3-dipolar cycloadditions of C,N-disubstituted aldonitrones to chalcones evidenced by NMR and X-ray analysis

Nivedita Acharjee · Avijit Banerji · Thierry Prangé

Received: 17 February 2010 / Accepted: 20 August 2010 / Published online: 21 September 2010

Abstract A DFT/B3LYP/6-31G* study was carried out to predict the regio- and stereoselectivities of 1,3-dipolar cycloadditions of C,N-disubstituted aldonitrones to chalcones in terms of FMO theory, DFT-based reactivity indices, and activation energy calculations. The structures of the resultant 2,3,4,5-tetrasubstituted isoxazolidines were determined by means of NMR spectroscopy and X-ray analysis.

Keywords Energy barrier · Electrophilicity index · NMR spectroscopy · X-ray structure determination

Introduction

Isoxazolidines are attractive intermediates for the synthesis of several natural products and biologically active compounds [1–4]. The synthesis of N,O-psiconucleosides has been recently designed on the basis of 1,3-dipolar cycloaddition (1,3-DC) of *C*-alkoxy carbonylnitrone to enol esters [5]. Several computational studies [6–10] have been carried out to explore the nature of the transition state and rationalize the observed regio- and stereoselectivities of nitrone cycloadditions. We have recently reported [11] the *exo*-stereoselective cycloaddition reaction of 1-pyrroline-1-oxide to chalcone by both experimental and theoretical approaches. We have previously reported cycloaddition reactions of C,N-disubstituted aldonitrones to substituted cinnamic acid amides [12] and β-nitrostyrenes [13]. When we carried out 1,3-DCs of these nitrones to chalcones, we observed that the product composition depends on the nature of the nitrogen substituent of the reacting nitrone. With this in mind, we became interested in rationalizing the observed regio- and stereoselectivities of these reactions in terms of FMO theory, DFT based reactivity indices, and activation energy calculations of the transition states.

N. Acharjee · A. Banerji (✉)
Centre of Advanced Studies on Natural Products Including Organic Synthesis, Department of Chemistry, University of Calcutta, 92, Acharya Prafulla Chandra Road, Kolkata 700009, India
e-mail: abnachem@rediffmail.com

T. Prangé
Laboratoire de Cristallographie et RMN Biologiques (UMR 8015 CNRS), Université Paris Descartes, 4, Av. de l'Observatoire, 75006 Paris, France

Results and discussion

Experimental results

Chalcones react with C,N-disubstituted aldonitrones to generate 2,3,4,5-tetrasubstituted isoxazolidines in a stereoselective manner. We have attempted to study the effect of changing the nitrogen substituent of the reacting nitrone with groups differing in electronic demand (Fig. 1). *C*-(4-Chlorophenyl)-*N*-phenyl nitrone (**1**) and *C*-phenyl-*N*-(4-chlorophenyl) nitrone (**2**) were prepared according to the existing procedure [2, 3] by heating the corresponding N-substituted hydroxylamines with the respective aldehydes in ethanol. *C*-(4-Chlorophenyl)-*N*-methyl nitrone (**3**) was obtained by a microwave-assisted procedure from *N*-methyl hydroxylamine hydrochloride and 4-chlorobenzaldehyde [14]. Chalcone (**4**) and anisalacetophenone (**5**) were prepared by mixed aldol condensations developed by Kohler and Chadwell [15]. The diastereomeric excesses were evaluated from the integration pattern (protons of the

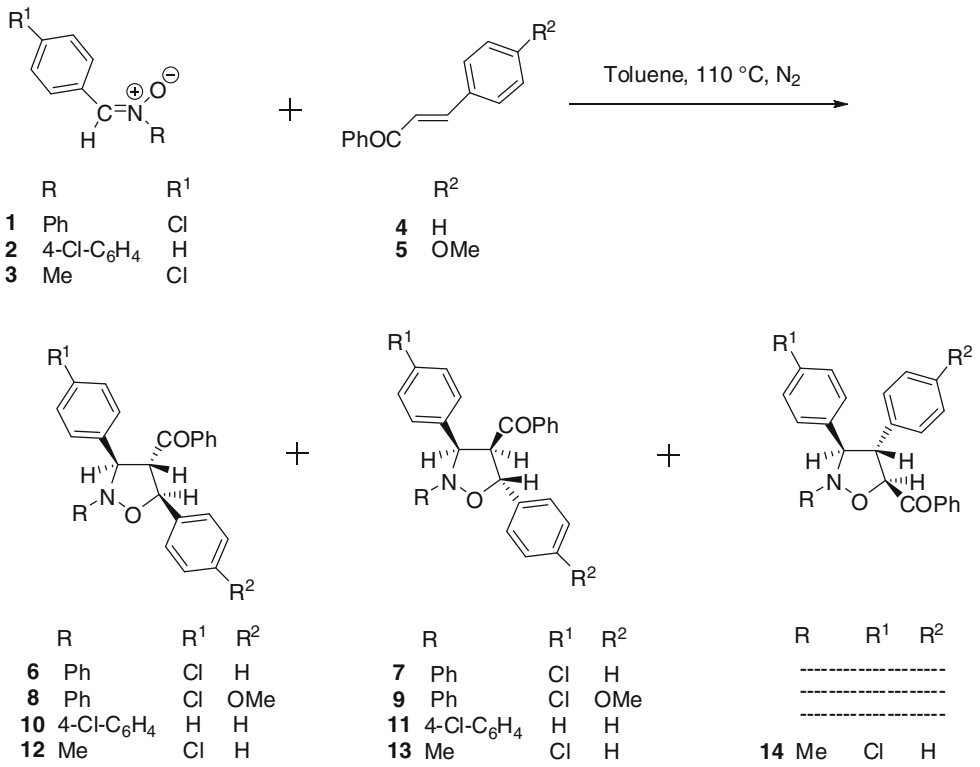

	R	R^1
1	Ph	Cl
2	4-Cl-C_6H_4	H
3	Me	Cl

	R^2
4	H
5	OMe

	R	R^1	R^2
6	Ph	Cl	H
8	Ph	Cl	OMe
10	4-Cl-C_6H_4	H	H
12	Me	Cl	H

	R	R^1	R^2
7	Ph	Cl	H
9	Ph	Cl	OMe
11	4-Cl-C_6H_4	H	H
13	Me	Cl	H

	R	R^1	R^2
	----------	----------	----------
	----------	----------	----------
	----------	----------	----------
14	Me	Cl	H

Fig. 1 1,3-Dipolar cycloadditions of C,N-disubstituted aldonitrones to α,β-unsaturated ketones

isoxazolidine ring of the cycloadducts) of 300 MHz ^{1}H NMR spectra of the crude reaction mixtures prior to column chromatography.

The structural analyses of the cycloadducts were carried out by means of ^{1}H, ^{13}C, and several 2D NMR spectroscopic techniques. 1,3-DC of **1** to **4** gives rise to two cycloadducts **6** and **7**. The 300-MHz ^{1}H NMR spectrum of the major cycloadduct **6** shows doublets at $\delta = 5.25$ ppm ($J = 7.2$ Hz) and 5.31 ppm ($J = 9.0$ Hz). A double doublet appears at $\delta = 4.45$ ppm with coupling constants of 7.2 and 9.0 Hz. This indicates that the proton signal at 4.45 ppm can be confidently assigned to H4 of the isoxazolidine ring. The major cycloadduct **8** generated from the reaction between **1** and **5** shows doublets at $\delta = 5.28$ ppm ($J = 7.2$ Hz) and 5.23 ppm ($J = 9.1$ Hz); the double doublet appears at 4.45 ppm. The doublet signal at 5.31 ppm in **6** is shielded to 5.23 ppm in **8** due to 4-methoxy substitution in ring D. Therefore, we can assign the doublet signals at $\delta = 5.31$ ppm and 5.23 ppm to H5 of the isoxazolidine rings in **6** and **8**. The H5 proton signal of the minor cycloadduct **7** at $\delta = 5.96$ ppm is shielded to 5.88 ppm in **9**. LR COSY couplings between H3 and H5 of **6** and **7** show that the corresponding *ortho* protons of the aromatic rings are attached to C3 and C5, thus indicating their benzylic disposition. The stereochemistry of the cycloadducts can be assigned from the coupling constants between H3 and H4 and that of H4 and H5. The coupling constants $J_{3,4}$ and $J_{4,5}$ of the minor cycloadducts **7** and **9** are large enough ($J_{3,4} = 10.1$ Hz, $J_{4,5} = 9.5$ Hz for compound **7** and $J_{3,4} = 10.0$ Hz, $J_{4,5} = 9.8$ Hz for compound **9**) to support a 3,4-*cis*-4,5-*trans* geometry of the isoxazolidine ring [12]. The stereochemistry of cycloadducts **6** and **8** was confirmed from single crystal X-ray analysis (Fig. 2). The structures are all *trans*, including the lone pair of nitrogen N2. Compound **6** has an intermediate envelope/twist conformation, whereas **8** shows a pure envelope conformation with the O1 atom out of the mean plane defined by the four other atoms.

The experimental results are collected in Table 1. The cycloaddition reaction of **2** to **4** gives rise to two diastereomeric cycloadducts **10** and **11**. We have then replaced the *N*-aryl group of **1** to *N*-methyl in **3**. Three cycloadducts, **12**, **13**, and **14**, are generated in a 78:8:14 ratio from 1,3-dipolar cycloaddition of **3** to **4** (Table 1). In the ^{1}H NMR spectra, chemical shifts of H3, H4, and H5 are sharply differentiated in three types of cycloadducts. The coupling constants $J_{3,4}$ and $J_{4,5}$ in **13** are large enough ($J_{3,4} = 10.2$ Hz, $J_{4,5} = 8.0$ Hz) to support the 3,4-*cis*-4,5-*trans* geometry of the isoxazolidine ring. Two-dimensional long-range COSY experiments reveal correlations between the benzylic proton and H3 for all three cycloadducts, **12**, **13**, and **14**. Such long-range correlations result from H5 and the benzylic protons in **12** and **13** as well as from the benzylic protons and H4 in **14**. In the regioisomer **14**, H3 and H5 are shielded by 0.18 and 0.23 ppm compared to **12**.

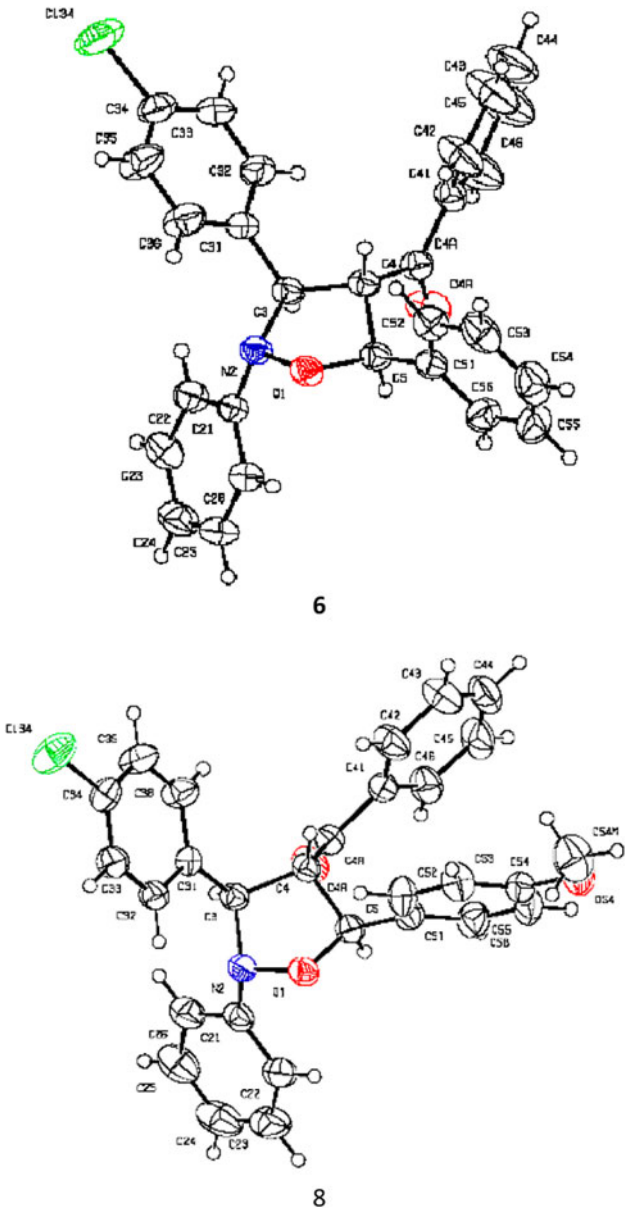

Fig. 2 ORTEP view of cycloadducts **6** and **8** (ellipsoids at the 40% probability level)

Table 1 Experimental results for 1,3-DCs of C,N-disubstituted aldonitrones to α,β-unsaturated compounds

Nitrone	Ketone	Reaction time (h)	Product ratios	Total conversion (%)
1	**4**	20	**6:7** = 87:13	69
1	**5**	20	**8:9** = 92:8	74
2	**4**	21	**10:11** = 90:10	71
3	**4**	17	**12:13:14** = 78:8:14	65

Table 2 DFT/B3LYP/6-31G* calculated HOMO and LUMO energies, and global properties of **1**, **3**, and **4**

	HO (a.u.)	LU (a.u.)	μ (a.u.)	η (a.u.)	S (a.u.)	ω (eV)
1	−0.207	−0.068	−0.138	0.139	3.597	1.864
3	−0.208	−0.056	−0.132	0.152	3.289	1.560
4	−0.233	−0.072	−0.153	0.161	3.106	1.978

Theoretical results

We selected the cycloaddition reactions of **1** and **3** to **4** as the reaction models for theoretical investigations.

Prediction of regioselectivity

From Houk's rule

The frontier orbital energies (calculated at DFT/B3LYP/6-31G* level of theory, Table 2) and the coefficients (calculated at HF/STO-3G level of theory) of **1**, **3**, and **4** are given in Fig. 3. HOMO/LUMO energy gaps of the reactants indicate a normal electron demand (NED) character (where $HOMO_{dipole}$–$LUMO_{dipolarphile}$ is the predominant interaction) for 1,3-DCs of **1** and **3** to **4**.

From Houk's rule, it is evident that the $HOMO_{dipole}$–$LUMO_{dipolarphile}$ interaction between the reactants will generate 4-benzoyl substituted isoxazolidines as the major cycloadducts for both the cycloaddition reactions. This agrees well with the experimental findings.

From NBO-derived charges

The NBO-derived charges of the reactive sites are collected in Table 3. The natural population analysis of **1** indicates that the oxygen and carbon atoms support negative charges of −0.517e and −0.009e. In case of **4**, C_α and C_β carry negative charges of −0.288e and −0.173e. Hence, the major isomers generated from the cycloaddition of **1** and **4** will be 4-benzoyl-substituted isoxazolidines with the oxygen atom of **1** (which is the most negative end of the dipole) attached to C_β (less negative end than C_α).

From DFT-based reactivity indices

The electronic chemical potential [16] μ is the index pointing to the direction of charge transfer (CT) within the system in its ground state. Global hardness [17] η specifies the resistance to the charge transfer process.

$$\mu \approx (\varepsilon_{HOMO} + \varepsilon_{LUMO})/2 \quad (1)$$

$$\eta \approx \varepsilon_{LUMO} - \varepsilon_{HOMO} \quad (2)$$

The electronic chemical potentials of **1** and **3** are higher than that of **4**. The chemical hardness of **4** is higher than that of **1** and **3**. This indicates that the CT at these reactions

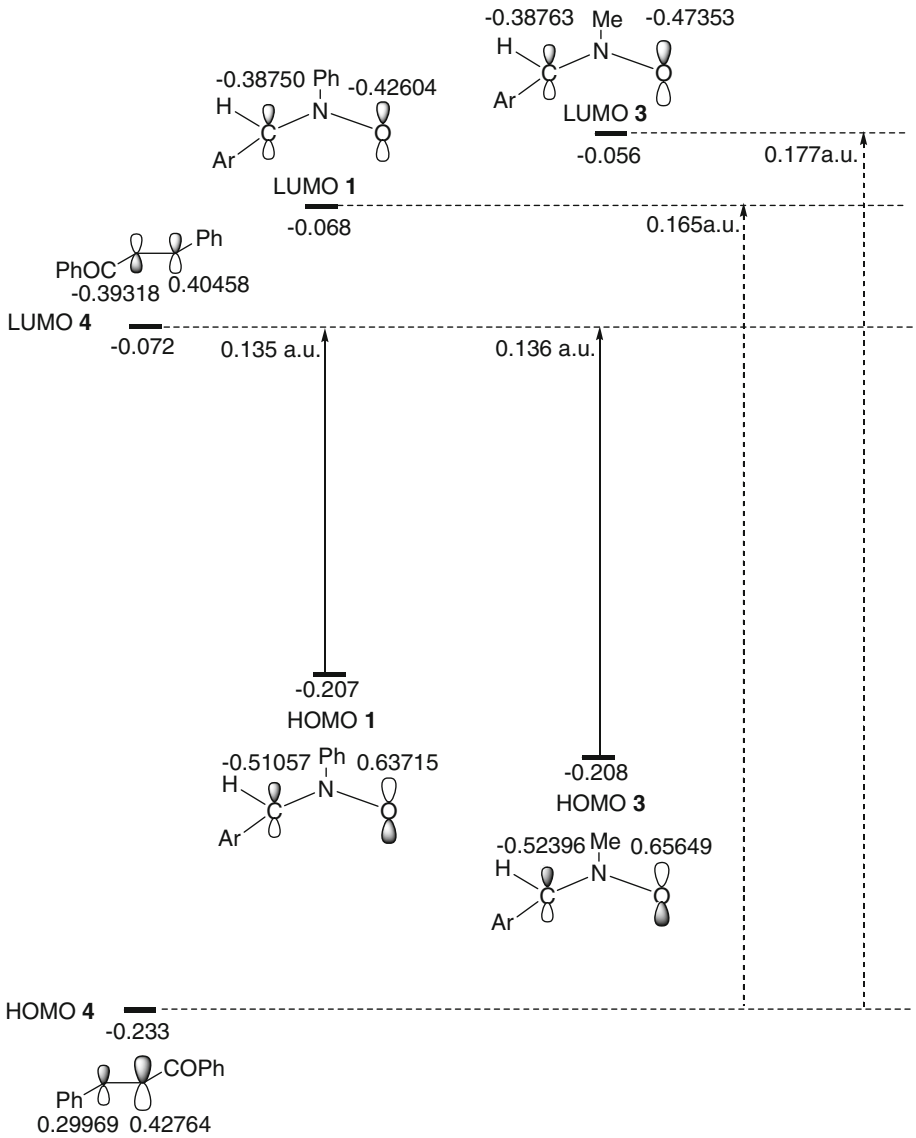

Fig. 3 HOMO and LUMO energies (in a.u.) (calculated at DFT/B3LYP/6-31G* level of theory) and the coefficients (calculated at HF/STO-3G level of theory) of the reacting termini of **1**, **3**, and **4** (not to the scale)

Table 3 DFT/B3LYP/6-31G* calculated local properties and natural charges (N) of the reactive sites in **1**, **3**, and **4**; k is the reactive site according to Fig. 4

	K	N	f_k^+	s^+ (a.u)	ω_k^+ (eV)	f_k^-	s^- (a.u.)
1	1	−0.517	0.099	0.356	0.185	0.217	0.781
	3	−0.009	0.123	0.442	0.229	0.125	0.450
3	1	−0.515	0.126	0.414	0.197	0.258	0.849
	3	−0.019	0.118	0.388	0.184	0.134	0.441
4	4	−0.288	0.036	0.112	0.071	0.089	0.276
	5	−0.173	0.119	0.370	0.235	0.050	0.155

will take place from the dipole to the dipolarophile, i.e., the NED character of the cycloaddition reactions. The global electrophilicity index ω [18–21] measures the stabilization in energy when the system acquires an additional electronic charge from the environment.

$$\omega = \mu^2/2\eta \tag{3}$$

For 1,3-DCs of **1** and **3** to **4**, the molecule with greater ω, i.e., the dipolarophile **4**, will act as the electrophile. This also suggests the NED character of both reactions. Small differences in the global electrophilicity indices of the reactants indicate a low polar character for both reactions.

The calculation of Fukui functions [22] of an atom in a molecule proves to be a useful criterion to characterize the reactive sites within a chemical species. For the two dipoles **1** and **3**, O1 ($k = 1$, Table 3) has higher f_k^- than C3 ($k = 3$, Table 3). ω_k^+ of C_β ($k = 5$, Table 3) is higher than that of C_α ($k = 4$, Table 3) in the dipolarophile **4**. Thus, the preferred interaction will take place between O1 of dipoles and C_β of **4**.

Table 4 DFT/B3LYP/6-31G* calculated softness matching index for 1,3-DCs of **1** to **4**, and **3** to **4**

	1 + **4**	**3** + **4**
$\Delta_{\text{4-oxophenyl substitution}}$ $[(s_{O1}^{-}-s_{C5}^{+})^2 + (s_{C3}^{-}-s_{C4}^{+})^2]$	0.283	0.338
$\Delta_{\text{5-oxophenyl substitution}}$ $[(s_{C3}^{-}-s_{C5}^{+})^2 + (s_{O1}^{-}-s_{C4}^{+})^2]$	0.454	0.548

Global softness S is represented as $S = 1/2\eta$ (4)

Regioselectivity can be analyzed in terms of the softness matching index Δ_{ij}^{kl} [23, 24], defined in terms of local softnesses by:

$$\Delta_{ij}^{kl} = \left(s_i^- - s_k^+\right)^2 + \left(s_j^- - s_l^+\right)^2 \quad (5)$$

where atoms i and j of the nucleophile interact with atoms k and l of the electrophile to give rise to the preferred regioisomer; s_i^-, s_k^+, s_j^-, and s_l^+ are the respective local softnesses of the reactive sites. Calculation of softness matching index ensures the simultaneous fulfillment of the local HSAB concept at the two reacting termini. The reaction pathway involving a lower value of Δ_{ij}^{kl} will be the favored one. For 1,3-DCs of **1** and **3** to **4**, Δ_{ij}^{kl} for the generation of 4-benzoyl substituted isoxazolidines is smaller compared to that for the generation of 5-benzoyl substituted isoxazolidines (Table 4). This suggests a preference for the generation of 4-benzoyl substituted isoxazolidines along the cycloaddition reactions and hence agrees well with the experimental results.

Activation energy calculations

(*Z*)-Isomers of both **1** and **3** are lower in energy than their (*E*)-counterparts by 34.85 and 30.54 kJ mol^{-1} at DFT/B3LYP/6-31G* level of theory. The preference for (*Z*)-configuration in both the nitrones is in agreement with NMR investigations [25, 26], dipole moment measurements [27, 28], and X-ray crystallographic studies [29]. The dipolarophile **4** exists exclusively in *trans* form. Transition state optimizations for the corresponding regio-attacks leading to the generation of 5-benzoyl substituted cycloadducts were attempted. However, such computations for reactions **1**–**4** and **3**–**4** lead to unrealistic structures and wrong activation energies of the transition states. Activation energy calculations of 1-pyrroline-1-oxide to chalcone also lead to similar observations [11]. In several calculations, the DFT method predicts a different regioisomer [10, 30]. Domingo et al. [31] have also reported the inability of DFT calculations to predict the regioselectivity of some nitrone cycloadditions. We are now left with activation energy calculations of the two stereoisomeric channels for the generation of 4-benzoyl substituted isoxazolidines from the investigated cycloadditions. They are related to the

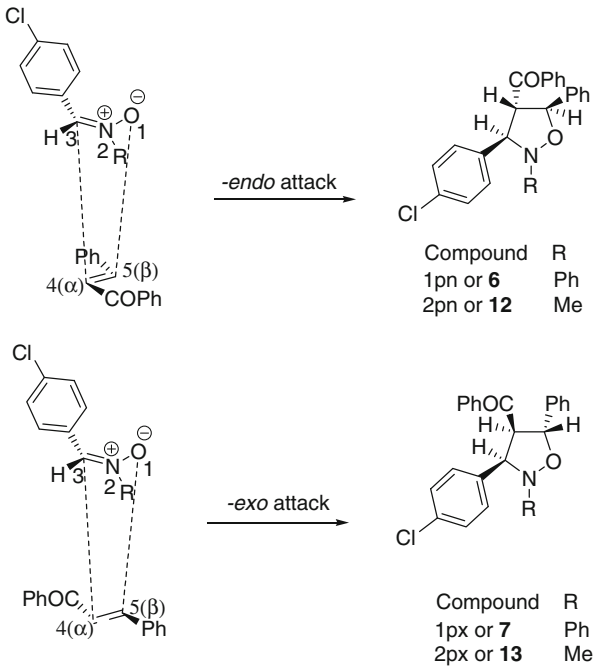

Fig. 4 *Endo* and *exo* attack on **1** and **3** by **4**

endo-carbonyl and *exo*-carbonyl approach modes of the dipolarophile **4** over the nitrogen atoms of the (*Z*)-nitrones **1** and **3** (Fig. 4).

The two reacting systems **1**–**4** and **3**–**4** have been denoted by prefixes 1 and 2, respectively, for the products and transition states. On grounds of structural symmetry, it is obvious that the calculations will be equivalent for both *re* and *si* faces of the nitrones **1** and **3**. We have focused our attention to one particular face, i.e., the *si* face of the nitrone. The naming symbols are coined according to a particular highlighted combination (**p**roducts/**t**ransition states, ***endo***/***exo***). In each case, the calculated C–C bond distance is longer than the C–O bond (Table 5). The index of Pauling's [32] partial bond order (PBO) has been calculated to comment on the bonding nature. Magnuson et al. [33] have reported their utilization in similar investigations. The comparable magnitudes of the PBOs for the transition states are within the range of concerted mechanism for both the cycloaddition reactions (Table 5).

Table 5 DFT/B3LYP/6-31G* calculated bond lengths and partial bond order (PBO) values of transition states

Transition state	r_{C-O} (Å)	$(PBO)_{C-O}$	r_{C-C} (Å)	$(PBO)_{C-C}$
1tn	2.109	0.119	2.149	0.154
1tx	2.092	0.127	2.163	0.150
2tn	1.982	0.165	2.152	0.146
2tx	1.936	0.196	2.093	0.182

Table 6 Total energies (a.u.) and relative energies (kJ mol^{-1}, in parentheses) relative to the reactants for 1,3-DCs of **1** to **4**, and **3** to **4**

	B3LYP/6-31G*	B3LYP/6-311++G**	B3LYP/6-31G* (in toluene)
1	−1,091.512317	−1,091.705883	−1,091.518683
3	−899.775870	−899.925976	−899.781311
4	−654.034373	−654.204907	−654.041028
1pn	−1,745.561900 (−39.934)	−1,745.916118 (−13.989)	−1,745.569975 (−26.948)
1px	−1,745.556387 (−25.459)	−1,745.910318 (1.239)	−1,745.565362 (−14.837)
1tn	−1,745.512553 (89.627)	−1,745.870635 (105.427)	−1,745.521760 (99.640)
1tx	−1,745.510125 (96.001)	−1,745.868045 (112.227)	−1,745.519911 (104.495)
2pn	−1,553.828363 (−47.574)	−1,554.137122 (−16.380)	−1,553.835431 (−34.373)
2px	−1,553.822688 (−32.674)	−1,554.132231 (−3.539)	−1,553.830525 (−21.492)
2tn	−1,553.775581 (91.005)	−1,554.088952 (110.090)	−1,553.784210 (100.108)
2tx	−1,553.768981 (108.333)	−1,554.082420 (127.240)	−1,553.777667 (117.286)

The *endo*-cycloadducts 1pn and 2pn are thermodynamically more stable compared to the *exo*-stereoisomers 1px and 2px, respectively (Table 6). The cycloaddition reaction between **1** and **4** is favored in the *endo*-reaction channel, being stabilized through an activation energy difference of 6.374 kJ mol^{-1} between 1tn and 1tx (Table 6). This is in concordance with the experimentally evaluated diastereomeric ratio of 1pn:1px ~87:13 (Table 1). The *exo*-stereoisomer **13** is obtained in least quantity from 1,3-DC of **3** to **4** (Table 1). The *exo*-transition state 2tx is destabilized by 17.328 kJ mol^{-1} relative to the *endo*-transition state 2tn. The computed activation energies of *exo*-transition states 1tx and 2tx differ by 12.332 kJ mol^{-1} and that of the *endo*-transition states 1tn and 2tn by 1.378 kJ mol^{-1}. This computational feature states that replacement of the *N*-phenyl group of **1** by *N*-methyl in **3** brings about a greater destabilization of the *exo*-carbonyl approach compared to that in case of the *endo*-carbonyl attack. The influence of the basis set was analyzed by comparing B3LYP/6-311++G** single-point energy calculations at the B3LYP/6-31G* geometry with the corresponding calculations of the B3LYP/6-31G* level of theory. The activation energy differences of the transition states are in good agreement. The inclusion of solvent effects gives rise to an increase of 8.4-10 kJ mol^{-1} in the energies relative to the gas phase calculations.

Computational methods

The geometries of the nitrones and chalcone have been optimized by Density Functional Theory with Becke's [34] three-parameter hybrid exchange functional in combination with the gradient-corrected correlation functional of Lee, Yang, and Parr [35] (B3LYP) using 6-31G* basis set. The electronic populations are computed from natural population analysis (NPA) [36] at DFT/B3LYP level of theory using 6-31G* basis set. The transition states have been localized at DFT/B3LYP/6-31G* level of theory. All the stationary points are definitely identified for minima (number of imaginary frequencies = 0) or transition states (number of imaginary frequencies = 1). Intrinsic reaction coordinate (IRC) calculations starting at the saddle points have been done to verify the connections between the transition states and their preceding and following minima along the reaction path. Solvent effects are considered by DFT/B3LYP/6-31G* single-point energy calculations at the gas phase geometries using the Polarized Continuum Model of Tomasi and coworkers [37, 38] (CPCM [39]) in toluene. The influence of the basis set has been studied by single-point energy calculations at the DFT/B3LYP/6-311++G** level of theory at the DFT/B3LYP/6-31G* optimized gas phase geometries. All calculations were carried out using a Gaussian 2003 [40] set of programs along with the graphical interface Gauss View 2003.

Experimental

Melting points were recorded on an electrically heated Kofler Block apparatus. UV spectra were recorded in dry acetonitrile using a Shimadzu UV-3101 PC spectrophotometer. IR spectra were recorded from KBr pellets using a Perkin-Elmer RX-9 FT-IR spectrophotometer. ^{1}H NMR and ^{13}C NMR spectra were recorded using a Bruker AV-300 NMR spectrometer at 300 and 75.5 MHz. ^{1}H NMR assignments were confirmed by decoupling, COSY, and COSY-LR experiments. ^{13}C NMR assignments were confirmed by DEPT and two-dimensional correlation experiments. Chemical shifts for ^{1}H NMR and ^{13}C NMR are reported in parts per million, downfield from tetramethylsilane (TMS). Mass spectra were recorded with a JEOL JMS600 mass spectrometer.

General procedure

A solution of 4.4 mmol nitrone and 6.6 mmol α,β-unsaturated ketone in 5 cm^3 dry thiophene-free toluene was refluxed under nitrogen atmosphere. The progress of each reaction was monitored by thin-layer chromatography (solvent system: petroleum ether:benzene 1:1). Toluene was removed under reduced pressure in a Büchi rotary evaporator from the post-reaction mixtures. The crude post-reaction mixtures were purified by column chromatography over neutral alumina (Activity I-II, Merck) using petroleum ether (60–80 °C) as the eluent. All solvents for thin-layer chromatography and column chromatography were distilled prior to use. Organic extracts were dried over anhydrous sodium sulfate.

(3α,4β,5α)-4-Benzoyl-3-(4-chlorophenyl)-2,5-diphenylisoxazolidine (**6**, $C_{28}H_{22}ClNO_2$)

White needle-shaped crystals; yield 0.99 g (51%); isolated from 10% benzene in petroleum ether eluates; $R_f = 0.55$ (silica gel, petroleum ether:benzene = 1:1); m.p.: 120 °C; UV–Vis (acetonitrile, $c = 5 \times 10^{-5}$ mol dm^{-3}): λ_{max} (log ε) = 245 (4.00) nm; IR (KBr): $\bar{\nu}$ = 3,045 (w), 1,677 (s), 1,594 (s), 1,487 (s), 825 (m), 755 (s), 695 (s) cm^{-1}; ^{1}H NMR (300 MHz, $CDCl_3$): $\delta = 5.25$ (d, $J = 7.2$ Hz, H3), 4.45 (dd, $J = 7.2$, 9.0 Hz, H4), 5.31 (d, $J = 9.0$ Hz, H5), 6.96 (d, $J = 7.7$ Hz, H2,6(A)), 6.90 (tt, $J = 7.3$, 1.0 Hz, H4(A)), 7.12–7.32 (m, H3,5(A), H2,3,5,6(B), H2,3,4,5,6(D)), 7.33–7.39 (m, H2,3,4,5,6(C)) ppm; ^{13}C NMR (75.5 MHz, $CDCl_3$): δ = 74.48 (C3), 69.41 (C4), 84.77 (C5), 151.35 (C1(A)), 114.34 (C2,6(A)), 127.90 (C3,5(A)), 122.06 (C4(A)), 136.29, 136.34 (C1(B), C1(D)), 133.60 (C4(B)), 140.06 (C1(C)), 133.74 (C4(C)), 126.77 (C2,6(D)), 128.91 (C4(D)), 129.19, 129.07, 128.79, 128.68, 128.48 (C2,6(B), C3,5(B), C2,6(C), C3,5(C), C3,5(D)), 196.40 (C=O) ppm; MS: *m/z* = 439 [$C_{28}H_{22}ClNO_2$, M^+], 334 [$C_{21}H_{17}ClNO$], 242 [$C_{15}H_{11}ClO$], 231 [$C_{13}H_{10}ClNO$], 216 [$C_{13}H_{11}ClN$], 209 [$C_{15}H_{12}OH^+$], 139, 131 [$C_9H_7O^+$], 111 [$C_6H_4Cl^+$], 105 [$C_7H_5O^+$], 91 [$C_7H_7^+$].

(3α,4α,5β)-4-Benzoyl-3-(4-chlorophenyl)-2,5-diphenylisoxazolidine (**7**, $C_{28}H_{22}ClNO_2$)

White crystals; yield 0.12 g (6%); isolated from 20% benzene in petroleum ether eluates from the mother liquor left after removing the crystals of **6**; $R_f = 0.50$ (silica gel, petroleum ether:benzene = 1:1); m.p.: 110 °C; IR (KBr): $\bar{\nu}$ = 3,043 (w), 1,668 (s), 1,591 (s), 1,486 (s), 827 (m), 756 (s), 695 (s) cm^{-1}; ^{1}H NMR (300 MHz, $CDCl_3$): $\delta = 5.05$ (d, $J = 10.1$ Hz, H3), 4.55 (dd, $J = 10.1$, 9.5 Hz, H4), 5.96 (d, $J = 9.5$ Hz, H5), 6.94 (d, $J = 7.8$ Hz, H2,6(A)), 6.91 (dist. t, H4(A)), 7.07–7.35 (m, H3,5(A), H2,3,5,6(B), H2,3,4,5,6(D)), 7.32–7.42 (m, H2,3,4,5,6(C)) ppm; ^{13}C NMR (75.5 MHz, $CDCl_3$): δ = 71.78 (C3), 66.31 (C4), 81.68 (C5), 149.07 (C1(A)), 115.90 (C2,6(A)), 127.98, 127.02 (C3,5(A), C2,6(D)), 122.72 (C4(A)), 133.50 (C1(B)), 134.51 (C4(B)), 139.92 (C1(C)), 134.02 (C4(C)), 135.96 (C1(D)), 129.12 (C4(D)), 129.28, 128.70, 128.58, 128.42, 128.18 (C2,6(B), C3,5(B), C2,6(C), C3,5(C), C3,5(D)), 195.81 (C=O) ppm; MS: *m/z* = 439 [$C_{28}H_{22}ClNO_2$, M^+], 231 [$C_{13}H_{10}ClNO$], 209 [$C_{15}H_{12}OH^+$], 139, 111 [$C_6H_4Cl^+$], 105 [$C_7H_5O^+$].

(3α,4β,5α)-4-Benzoyl-3-(4-chlorophenyl)-5-(4-methoxyphenyl)-2-phenylisoxazolidine (**8**, $C_{29}H_{24}ClNO_3$)

White crystals; yield 1.11 g (54%); isolated from 10% benzene in petroleum ether eluates; $R_f = 0.42$ (silica gel, petroleum ether:benzene = 1:1); m.p.: 140 °C; UV–Vis (acetonitrile, $c = 5 \times 10^{-5}$ mol dm^{-3}): λ_{max} (ε) = 231.5 (4.25) nm; IR (KBr): $\bar{\nu}$ = 3,054 (w), 1,676 (s), 1,597 (s), 1,483 (s), 1,249 (s), 827 (m), 756 (s), 694 (s) cm^{-1}; ^{1}H NMR (300 MHz, $CDCl_3$): $\delta = 3.69$ (s, OCH_3), 5.28 (d, $J = 7.1$ Hz, H3), 4.45 (dd, $J = 7.1$, 9.1 Hz, H4), 5.23 (d, $J = 9.1$ Hz, H5), 6.96 (d, $J = 7.7$ Hz, H2,6(A)), 7.13 (dist. t, H3,5(A)), 6.89 (tt, $J = 7.3$, 1.0 Hz, H4(A)), 7.16–7.40 (H2,3,5,6(B), H2,3,4,5,6(C), H2,6(D)), 6.76 (d, $J = 8.8$ Hz, H3,5(D)) ppm; ^{13}C NMR (75.5 MHz, $CDCl_3$): δ = 55.30 (OCH_3), 74.42 (C3), 69.28 (C4), 84.77 (C5), 151.48 (C1(A)), 114.19, 114.17 (C2,6(A), C3,5(D)), 127.82 (C3,5(A)), 121.90 (C4(A)), 136.29 (C1(B)), 133.51 (C4(B)), 140.26 (C1(C)), 133.70 (C4(C)), 127.91 (C1(D)), 160.08 (C4(D)), 129.17, 129.06, 128.69, 128.49, 128.27 (C2,6(B), C3,5(B), C2,6(C), C3,5(C), C2,6(D)), 196.40 (C=O) ppm; MS: *m/z* = 469 [$C_{29}H_{24}ClNO_3$, M^+], 231 [$C_{13}H_{10}ClNO$], 239 [$C_{16}H_{14}O_2H^+$], 139, 111 [$C_6H_4Cl^+$], 91 [$C_7H_7^+$].

(3α,4α,5β)-4-Benzoyl-3-(4-chlorophenyl)-5-(4-methoxyphenyl)-2-phenylisoxazolidine (**9**, $C_{29}H_{24}ClNO_3$)

White amorphous powder; yield 0.14 g (7%); isolated from 20% benzene in petroleum ether eluates from the mother liquor left after removing the crystals of **8**; $R_f = 0.36$ (silica gel, petroleum ether:benzene = 1:1); IR (KBr): $\bar{\nu}$ = 3,050 (w), 1,674 (s), 1,596 (s), 1,480 (s), 1,250 (s), 828 (m), 756 (s), 695 (s) cm^{-1}; ^{1}H NMR (300 MHz, $CDCl_3$): $\delta = 3.72$ (s, OCH_3), 5.04 (d, $J = 10.0$ Hz, H3), 4.55 (dd, $J = 10.0$, 9.8 Hz, H4), 5.88 (d, $J = 9.8$ Hz, H5), 6.95 (d, $J = 7.8$ Hz, H2,6(A)), 6.92 (dist. t, H4(A)), 7.09 (dist. t, H3,5(A)), 7.14–7.38 (H2,3,5,6(B), H2,3,4,5,6(C) H2,6(D)), 6.72 (d, $J = 8.7$ Hz, H3,5(D)) ppm; ^{13}C NMR (75.5 MHz, $CDCl_3$): δ = 54.99 (OCH_3), 71.74 (C3), 66.18 (C4), 81.65 (C5), 149.15 (C1(A)), 115.79 (C2,6(A)), 127.87 (C3,5(A)), 122.52 (C4(A)), 133.51 (C1(B)), 134.48 (C4(B)), 140.11 (C1(C)), 133.96 (C4(C)), 127.61 (C1(D)), 114.43 (C3,5(D)), 160.32 (C4(D)), 129.25, 128.68, 128.45, 128.22, 128.02 (C2,6(B), C3,5(B), C2,6(C), C3,5(C), C2,6(D)), 195.82 (C=O) ppm; MS: *m/z* = 469 [$C_{29}H_{24}ClNO_3$, M^+], 231 [$C_{13}H_{10}ClNO$], 239 [$C_{16}H_{14}O_2H^+$], 139, 111 [$C_6H_4Cl^+$].

(3α,4β,5α)-4-Benzoyl-2-(4-chlorophenyl)-3,5-diphenylisoxazolidine (**10**, $C_{28}H_{22}ClNO_2$)
White crystals; yield 1.01 g (52%); isolated from 10% benzene in petroleum ether eluates; $R_f = 0.54$ (silica gel, petroleum ether:benzene = 1:1); m.p.: 138 °C; IR (KBr): $\bar{\nu} = 3{,}057$ (w), 1,670 (s), 1,590 (s), 1,484 (s), 838 (m), 754 (s), 696 (s) cm^{-1}; ^1H NMR (300 MHz, $CDCl_3$): $\delta = 5.27$ (d, $J = 7.2$ Hz, H3), 4.59 (dd, $J = 7.2$, 9.0 Hz, H4), 5.38 (d, $J = 9.0$ Hz, H5), 6.99 (d, $J = 9.0$ Hz, H2,6(A)), 7.21 (d, $J = 9.0$ Hz, H3,5(A)), 7.24–7.50 (m, H2,3,4,5,6(B), H2,3,4,5,6(C), H2,3,4,5,6(D)) ppm; ^{13}C NMR (75.5 MHz, $CDCl_3$): $\delta = 75.32$ (C3), 69.37 (C4), 84.79 (C5), 150.18 (C1(A)), 115.66 (C2,6(A)), 126.44, 126.74 (C3,5(A), C2,6(D)), 126.80 (C4(A)), 136.23, 136.29 (C1(B), C1(D)), 127.97 (C4(B)), 140.99 (C1(C)), 133.68 (C4(C)), 128.77 (C4(D)), 128.92, 129.09, 128.78, 128.70, 128.41 (C2,6(B), C3,5(B), C2,6(C), C3,5(C) C3,5(D)), 196.55 (C=O) ppm; MS: $m/z = 439$ [$C_{28}H_{22}ClNO_2$, M^+], 334 [$C_{21}H_{17}ClNO$], 231 [$C_{13}H_{10}ClNO$], 216 [$C_{13}H_{11}ClN$], 209 [$C_{15}H_{12}OH^+$], 131 [$C_9H_7O^+$], 91 [$C_7H_7^+$].

(3α,4α,5β)-4-Benzoyl-2-(4-chlorophenyl)-3,5-diphenylisoxazolidine (**11**, $C_{28}H_{22}ClNO_2$)
White powder; yield 0.12 g (6%); isolated from 10% benzene in petroleum ether eluates from the mother liquor after removal of the cycloadduct **10**; $R_f = 0.50$ (silica gel, petroleum ether:benzene = 1:1); IR (KBr): = 3,055 (w), 1,668 (s), 1,589 (s), 1,482 (s), 839 (m), 756 (s), 697 (s) cm^{-1}; ^1H NMR (300 MHz, $CDCl_3$): $\delta = 4.97$ (d, $J = 10.2$ Hz, H3), 4.88 (dd, $J = 10.2$, 9.4 Hz, H4), 5.99 (d, $J = 9.4$ Hz, H5), 6.94 (d, $J = 9.1$Hz, H2,6(A)), 7.17 (d, $J = 9.1$ Hz, H3,5(A)), 7.20–7.52 (m, H2,3,4,5,6(B), H2,3,4,5,6(C), H2,3,4,5,6(D)) ppm; ^{13}C NMR (75.5 MHz, $CDCl_3$): $\delta =$ 72.61 (C3), 66.20 (C4), 81.70 (C5), 148.00 (C1(A)), 116.97 (C2,6(A)), 126.54 (C3,5(A)), 127.45 (C4(A)), 133.46 (C1(B)), 128.89 (C4(B)), 140.86 (C1(C)), 133.98 (C4(C)), 135.91 (C1(D)), 127.68 (C2,6(D)), 129.92 (C4(D)), 129.22, 129.04, 128.89, 128.45, 128.09 (C2,6(B), C3,5(B), C2,6(C), C3,5(C), C3,5(D)), 195.97 (C=O) ppm; MS: $m/z = 439$ [$C_{28}H_{22}ClNO_2$, M^+], 231 [$C_{13}H_{10}ClNO$], 209 [$C_{15}H_{12}OH^+$], 131 [$C_9H_7O^+$], 105 [$C_7H_5O^+$], 91 [$C_7H_7^+$].

(3α,4β,5α)-4-Benzoyl-3-(4-chlorophenyl)-2-methyl-5-phenylisoxazolidine (**12**, $C_{23}H_{20}ClNO_2$)
White amorphous powder; yield 0.81 g (49%); isolated from 10% benzene in petroleum ether eluates; $R_f = 0.60$ (silica gel, benzene:ethylacetate = 4:1); ^1H NMR (300 MHz, $CDCl_3$): $\delta = 2.95$ (NCH_3), 4.18 (d, $J = 8.4$ Hz, H3), 4.32 (dd, $J = 8.4$, 6.7 Hz, H4), 5.35 (d, $J = 6.7$ Hz, H5), 7.06 (d, $J = 7.7$ Hz, H2,6(B)), 7.19–7.22 (m, H3,5(B), H2,3,4,5,6 (D)), 7.40-7.62 (m, H2,3,4,5,6(C)) ppm; ^{13}C NMR (75.5 MHz, $CDCl_3$): $\delta = 43.40$ (NCH_3), 68.31 (C3), 54.32 (C4), 82.07 (C5), 136.29, 136.79, (C1(B), C1(C)), 134.78 (C4(B)), 133.82 (C4(C)), 137.81 (C1(D)), 128.21 (C4(D)), 129.48, 129.32, 128.68, 128.57, 128.39, 128.34 (C2,6(B), C3,5(B), C2,6(C), C3,5(C), C2,6(D), C3,5(D)), 197.48 (C=O) ppm; MS: $m/z = 377$ [$C_{23}H_{20}ClNO_2$, M^+], 242 [$C_{15}H_{11}ClO$], 209 [$C_{15}H_{12}OH^+$], 167 [C_8H_8ClNO-2H·], 105 [$C_7H_5O^+$], 91 [$C_7H_7^+$].

(3α,4α,5β)-4-Benzoyl-3-(4-chlorophenyl)-2-methyl-5-phenylisoxazolidine (**13**, $C_{23}H_{20}ClNO_2$)
White powder; yield 0.09 g (5.5%); isolated from 10% benzene in petroleum ether eluates; $R_f = 0.54$ (silica gel, benzene:ethylacetate = 4:1); ^1H NMR (300 MHz, $CDCl_3$): $\delta = 2.72$ (NCH_3), 4.00 (d, $J = 10.2$ Hz, H3), 4.40 (dd, $J = 10.2$, 8.0 Hz, H4), 5.86 (dd, $J = 8.0$ Hz, H5), 7.04 (d, $J = 7.8$ Hz, H2,6(B)), 7.14–7.16 (m, H3,5(B), H2,3,4,5, 6(D)), 7.32–7.57 (m, H2,3,4,5,6(C)) ppm; ^{13}C NMR (75.5 MHz, $CDCl_3$): $\delta = 42.82$ (NCH_3), 67.16 (C3), 50.35 (C4), 81.50 (C5), 134.79, 134.10 (C1(B), C4(B)), 136.62 (C1(C)), 133.55 (C4(C)), 137.48 (C1(D)), 128.36 (C4(D)), 129.37, 128.96, 128.47, 128.36, 128.07, 128.02 (C2,6(B), C3,5(B), C2,6(C), C3,5(C), C2,6(D), C3,5(D)), 196.42 (C=O) ppm; MS: $m/z = 377$ [$C_{23}H_{20}ClNO_2$, M^+], 242 [$C_{15}H_{11}ClO$], 209 [$C_{15}H_{12}OH^+$], 167 [C_8H_8ClNO-2H·], 105 [$C_7H_5O^+$].

(3α,4β,5α)-5-Benzoyl-3-(4-chlorophenyl)-2-methyl-4-phenylisoxazolidine (**14**, $C_{23}H_{20}ClNO_2$)
White powder; yield 0.12 g (7.5%); isolated from 20% benzene in petroleum ether:benzene (4:1) eluates; $R_f = 0.65$ (silica gel, benzene:ethylacetate = 4:1); ^1H NMR (300 MHz, $CDCl_3$): $\delta = 2.76$ (NCH_3), 4.00 (d, $J = 8.6$ Hz, H3), 4.20 (dd, $J = 8.6$, 4.7 Hz, H4), 5.12 (d, $J = 4.7$ Hz, H5), 7.00 (d, $J = 7.7$ Hz, H2,6(B)), 7.10–7.40 (m, H3,5(B), H2,3,4,5,6(C), H2,3,4,5,6(D)) ppm; ^{13}C NMR (75.5 MHz, $CDCl_3$): $\delta = 42.56$ (NCH_3), 70.78 (C3), 51.81 (C4), 81.12 (C5), 135.30 (C1(B)), 133.72 (C4(B)), 137.71, 138.02 (C1(C), C1(D)), 133.12 (C4(C)), 128.01 (C4(D)), 129.61, 129.56, 129.42, 129.06, 128.58, 128.20 (C2,6(B), C3,5(B), C2,6(C), C3,5(C), C2,6(D), C3,5(D)), 196.20 (C=O) ppm; MS: $m/z = 377$ [$C_{23}H_{20}ClNO_2$, M^+], 209 [$C_{15}H_{12}OH^+$], 167 [C_8H_8ClNO-2H·], 105 [$C_7H_5O^+$].

X-ray structure determination

Suitable crystals of sizes 0.3 × 0.3 × 0.15 mm for compound **6** and 0.4 × 0.2 × 0.2 mm for compound **8** were dispersed in oil (Nujol) and fished with a nylon loop under microscope. They were directly mounted on a CCD Kappa Nonius diffractometer operating with Mo Kα radiation ($\lambda = 0.7107$ Å). The measurements were recorded at 291 K for both compounds. Refinement was done with the *SHELXL* program [41], using isotropic then anisotropic thermal parameters. The hydrogen atoms were localized on Fourier difference maps and introduced with

an isotropic thermal factor equal to that of the bonded atom.

6: Space group monoclinic, $P21/c$; $Z = 4$; Cell parameters: $a = 10.443(2)$ Å, $b = 20.542(2)$ Å, $c = 11.028(2)$ Å, $\alpha = \gamma = 90°$, $\beta = 103.51(1)°$; $V = 2{,}300.3(6)$ Å^3.

8: Space group triclinic $P1$; $Z = 2$; Cell parameters: $a = 9.984(2)$ Å, $b = 11.347(2)$ Å, $c = 11.646(2)$ Å, $\alpha = 99.762(5)°$, $\beta = 105.486(5)°$; $\gamma = 101.499(5)°$, $V = 1{,}210.8(4)$ Å^3.

These X-ray data have been deposited at the Cambridge Structural Data Centre under CCDC numbers 755889 and 755890. The data can be obtained free of charge via www.ccdc.cam.ac.uk/data_request/cif or by e-mailing data_request@ccdc.cam.ac.uk, or by contacting The Cambridge Crystallographic Data Centre, 12, Union Road, Cambridge CB2 1EZ, UK; fax: +441223 336033.

Acknowledgments Nivedita Acharjee is thankful to the Council of Scientific and Industrial research, New Delhi (India), for financial support and the University of Calcutta for laboratory and computational facilities. We are thankful to Prof. Manas Banerjee of Burdwan University for some informative discussions.

References

1. Merino P (2004) In: Padwa A (ed) Science of synthesis, chapter 13 (Nitrones and Analogues). Georg Thieme Verlag, Stuttgart, Germany, 27:511
2. Torssell KBG (1988) Nitrile oxides, nitrones and nitronates in organic synthesis. VCH, Weinheim, New York
3. Padwa A, Pearson WH (2002) Synthetic applications of 1, 3-dipolar cycloaddition chemistry towards heterocycles and natural products. Wiley, New York
4. Chiacchio U, Rescifina A, Iannazzo D, Piperno A, Romeo R, Borrello L, Sciortino MT, Balestrieri E, Macchi B, Mastino A, Romeo G (2007) J Med Chem 50:3747
5. Iannazzo D, Piperno A, Pistarà V, Rescifina A, Romeo R (2002) Tetrahedron 58:581
6. Merino P, Revuelta J, Tejero T, Chiacchio U, Rescifina A, Romeo G (2003) Tetrahedron 59:3581
7. Benchouk W, Mekelleche SM (2008) J Mol Struct Theochem 852:46
8. Barba C, Carmona D, Garcia JI, Lamata MP, Mayoral JA, Salvatella L, Viguri F (2006) J Org Chem 71:9831
9. Domingo LR, Aurell MJ, Arno M, Saez JA (2007) J Mol Struct Theochem 811:125
10. Merino P, Tejero T, Chiacchio U, Romeo G, Rescifina A (2007) Tetrahedron 63:1448
11. Acharjee N, Das TK, Banerji A, Banerjee M, Prangé T (2010) J Phys Org Chem. doi:10.1002/poc.1690
12. Banerji A, Maiti KK, Haldar S, Mukhopadhyay C, Banerji J, Prangé T, Neuman A (2000) Monatsh Chem 131:901
13. Banerji A, Gupta M, Biswas PK, Prangé T, Neuman A (2007) J Heterocycl Chem 44:1045
14. Banerji A, Biswas PK, Sengupta P, Dasgupta S, Gupta M (2004) Indian J Chem 43B:880
15. Gilman H (ed) (1941) Org Synth Coll Vol, John Wiley, New York 1:78
16. Parr RG, Yang W (1989) Density functional theory of atoms and molecules. Oxford University Press, NewYork
17. Parr RG, Pearson RG (1983) J Am Chem Soc 105:7512
18. Parr RG, Szentpaly LV, Liu S (1999) J Am Chem Soc 121:1922
19. Domingo LR, Aurell MJ, Perez P, Contreras R (2002) Tetrahedron 58:4417
20. Perez P, Domingo LR, Aurell MJ, Contreras R (2003) Tetrahedron 59:3117
21. Chattaraj PK, Sarkar U, Roy DR (2006) Chem Rev 106:2065
22. Yang W, Mortier WJ (1986) J Am Chem Soc 108:5708
23. Chandra AK, Nguyen MT (1997) J Chem Soc Perkin Trans 2:1415
24. Zhang YL, Yang ZZ (2000) J Mol Struct Theochem 496:139
25. Koyano K, Suzuki H (1968) Tetrahedron Lett 15:1859
26. Koyano K, Suzuki H (1969) Bull Soc Chem Japan 42:3306
27. Taylar TWJ, Sutton LE (1931) J Chem Soc, p 2190
28. Taylar TWJ, Sutton LE (1933) J Chem Soc, p 63
29. Foltino K, Lipscomb WN, Jerslev B (1963) Acta Chem Scand 17:2138
30. Cossio FP, Morao I, Jiao H, Schleyer PVR (1999) J Am Chem Soc 121:6737
31. Carda M, Portolés R, Murga J, Uriel S, Marco JA, Domingo LR, Zaragoźa RJ, Röper H (2000) J Org Chem 65:7000
32. Pauling L (1960) The nature of chemical bond, 3rd edn. Cornell University, Ithaca, New York, p 239
33. Magnuson EC, Pranata J (1998) J Comput Chem 19:1795
34. Becke AD (1993) J Chem Phys 98:5648
35. Lee C, Yang W, Parr RG (1988) Phys Rev B 37:785
36. Reed AE, Weinhold F (1983) J Chem Phys 78:4066
37. Miertus S, Tomasi J (1982) Chem Phys 65:239
38. Miertus S, Scrocco E, Tomasi J (1981) Chem Phys 55:117
39. Barone V, Cossi M (1998) J Phys Chem A 102:1995
40. Frisch MJ, Trucks GW, Schlegel HB, Scuseria GE, Robb MA, Cheeseman JR, Montgomery JA Jr, Vreven T, Kudin KN, Burant JC, Millam JM, Iyengar SS, Tomasi J, Barone V, Mennucci B, Cossi M, Scalmani G, Rega N, Petersson GA, Nakatsuji H, Hada M, Ehara M, Toyota K, Fukuda R, Hasegawa J, Ishida M, Nakajima T, Honda Y, Kitao O, Nakai H, Klene M, Li X, Knox JE, Hratchian HP, Cross JB, Adamo C, Jaramillo J, Gomperts R, Stratmann RE, Yazyev O, Austin AJ, Cammi R, Pomelli C, Ochterski JW, Ayala PY, Morokuma K, Voth GA, Salvador P, Dannenberg JJ, Zakrzewski VG, Dapprich S, Daniels AD, Strain MC, Farkas O, Malick DK, Rabuck AD, Raghavachari K, Foresman JB, Ortiz JV, Cui Q, Baboul AG, Clifford S, Cioslowski J, Stefanov BB, Liu G, Liashenko A, Piskorz P, Komaromi I, Martin RL, Fox DJ, Keith T, Al-Laham MA, Peng CY, Nanayakkara A, Challacombe M, Gill PMW, Johnson B, Chen W, Wong MW, Gonzalez C, Pople JA (2004) Gaussian 03, Rev. D.01. Gaussian Inc, Wallingford, CT
41. Sheldrick GM, Schneider TR (1997) Methods Enzymol 277: 319